

Stemming the Flow: MitoNEET Redox-Selectively Controls VDAC Gating

Colin H. Lipper^{a,1}, Jason T. Stofleth^{a,1}, Fang Bai^b, Yang-Sung Sohn^c, Susmita Roy^b, Ron Mittler^d, Rachel Nechushtai^c, Jose N. Onuchic^b, Patricia A. Jennings^a.

Supplemental Information Appendix

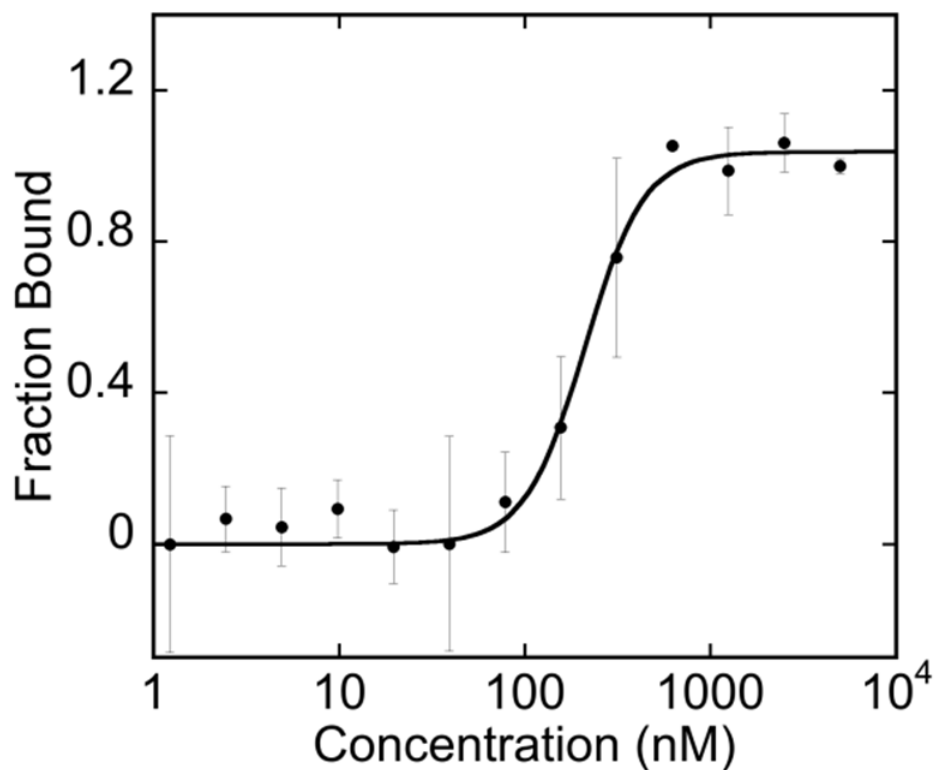


Figure S1. MST measurement of mNT binding to VDAC nanodisc. MST analysis of a serial dilution of mNT binding to fluorescently labeled VDAC assembled in nanodiscs under oxidizing conditions results in a measured K_d of 210 ± 15 nM.

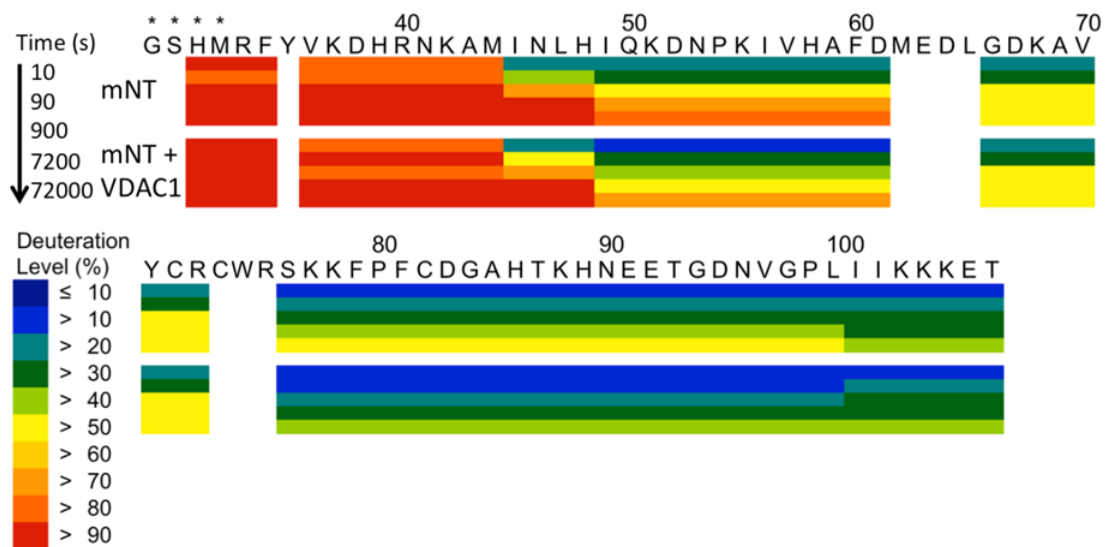


Figure S2. Heat map representation of time-dependent deuterium incorporation for mNT in complex VDAC. For time points of 10 s, 90 s, 900 s, 7200 s, and 72000 s, peptide probes are assigned to the primary sequence and color-coded to denote the percentage of deuterium incorporated. The top time course is mNT alone and the bottom is mNT in complex with VDAC.

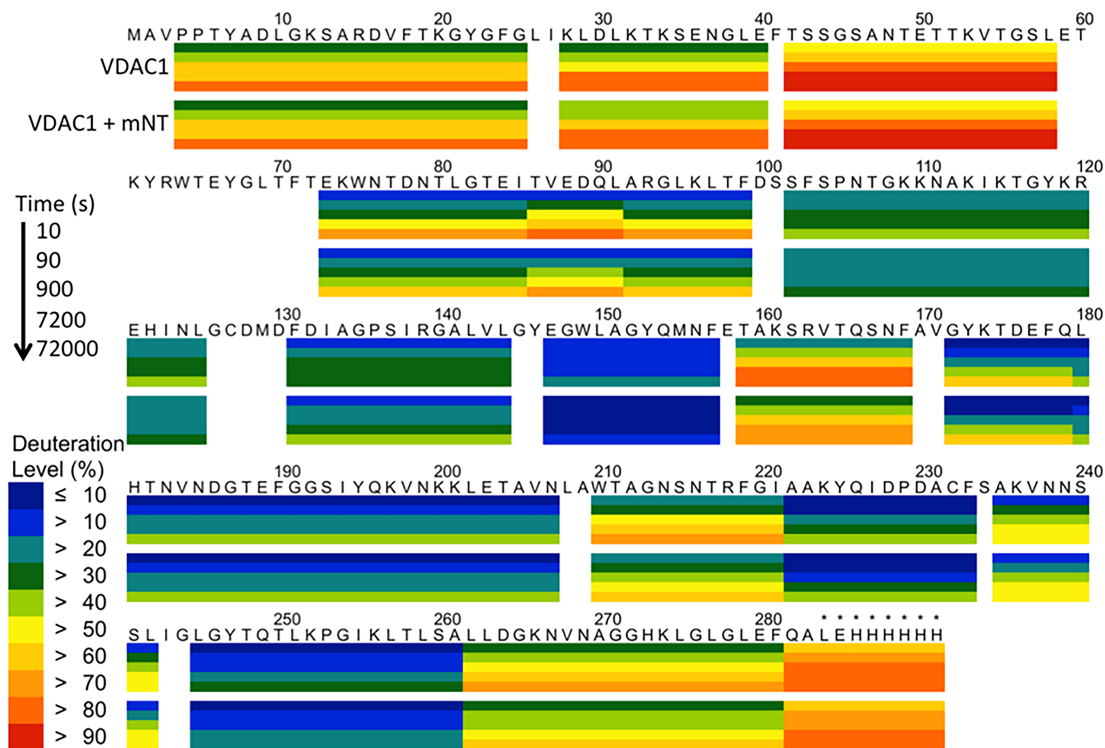


Figure S3. Heat map representation of time-dependent deuterium incorporation for VDAC in complex mNT. For time points of 10 s, 90 s, 900 s, 7200 s, and 72000 s, peptide probes are assigned to the primary sequence and color-coded to denote the percentage of deuterium incorporated. The top time course is VDAC alone and the bottom is VDAC in complex with mNT.

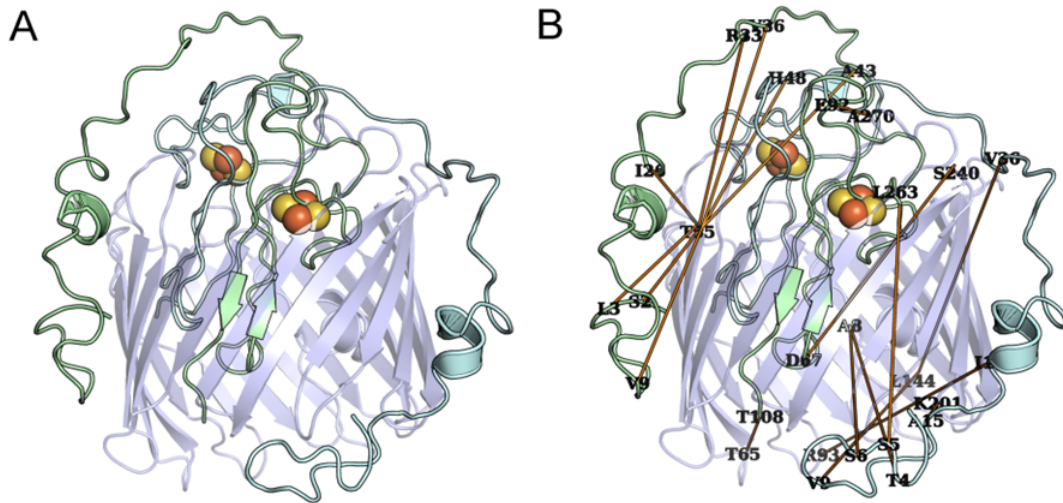


Figure S4. The images of modeled binding complex of mNT-VDAC (A) with DCA constraints (B). The pale green and pale cyan cartoons are different chains of mNT, and light purple cartoon is VDAC. Orange lines indicate the top 20 coevolving residue pairs.

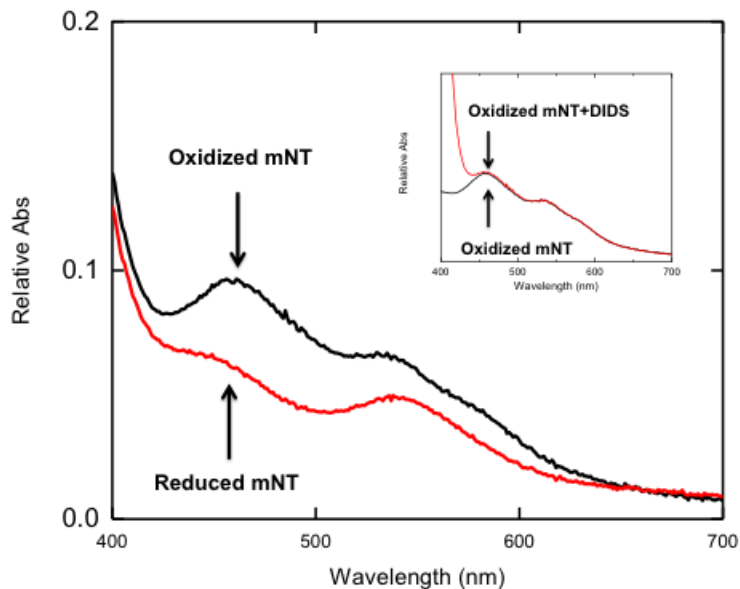


Figure S5: DIDS does not alter the Redox-State of mNT. Optical spectra of mNT as isolated is oxidized as evidenced by the absorbance peaks at 458 and 530 nm. The absorption spectra of the reduced mNT exhibits the expected changes for the reduction of the 2Fe-2S centers. (INSET) Addition of DIDS does not alter the redox state of mNT as evidenced by the retention of the characteristic absorption maximums at 458 and 530 nm.

Human	1	MAVPPPTYADLGKSARDVFTKGYGFGLIKLDLKTKE ENGLEFTSSGSANETTTKVTGSLET
Sheep	1	MAVPPPTYADLGKSARDVFTKGYGFGLIKLDLKTKE ENGLEFTSSGSANETTTKVTGSLET
Human	61	KYRWTEYGLTFTEKWNTDNTLGTEITVEDQLARGLKLTFDSSFSPNTGKKNAKIKTGYKR
Sheep	61	KYRWTEYGLTFTEKWNTDNTLGTEITVEDQLARGLKLTFDSSFSPNTGKKNAKIKTGYKR
Human	121	EHINLGCDMDFDIAGPSIRGALVLGYEGWLAGYQMNFE TAKSRVTSNFAVGYKTDEFQL
Sheep	121	EHINLGCDVDFDIAGPSIRGALVLGYEGWLAGYQMNFE TAKSRVTSNFAVGYKTDEFQL
Human	181	HTNVNDGTEFGGSYQKVNKLETAVNLAWTAGNSNTRFGIAAKYQIDPDACFS AKVNNS
Sheep	181	HTNVNDGTEFGGSYQKVNKLETAVNLAWTAGNSNTRFGIAAKYQIDPDACSS AKVNNS
Human	241	SLIGLGYTQTLKPGIKLTL SALLDGKNVNAGGHKLGLEFQA
Sheep	241	SLIGLGYTQTLKPGIKLTL SALLDGKNVNAGGHKLGLEFQA

Figure S6. The sequence alignment for human VDAC1 (Accession NP_003365.1) to sheep VDAC1 (Accession NP_001119824.1) shows over 99% sequence identity with 239 out of 241 residues being the same. Residues varying between the two orthologs are numbers 129 and 174.

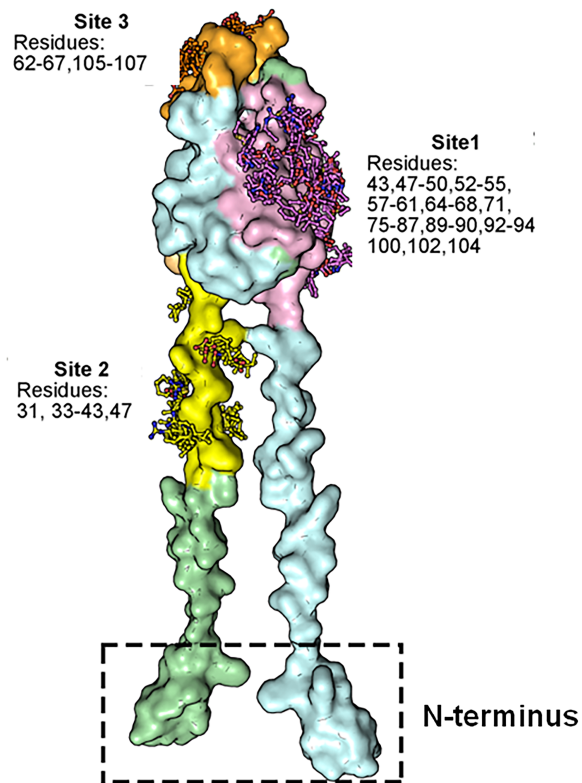


Figure S7. Candidate binding sites for VDAC interaction are identified for mNT. The stick-ball models represent the energetically favorable bound fragment-molecular probes, the corresponding surface highlighted with the similar color of probes are identified candidate binding sites.

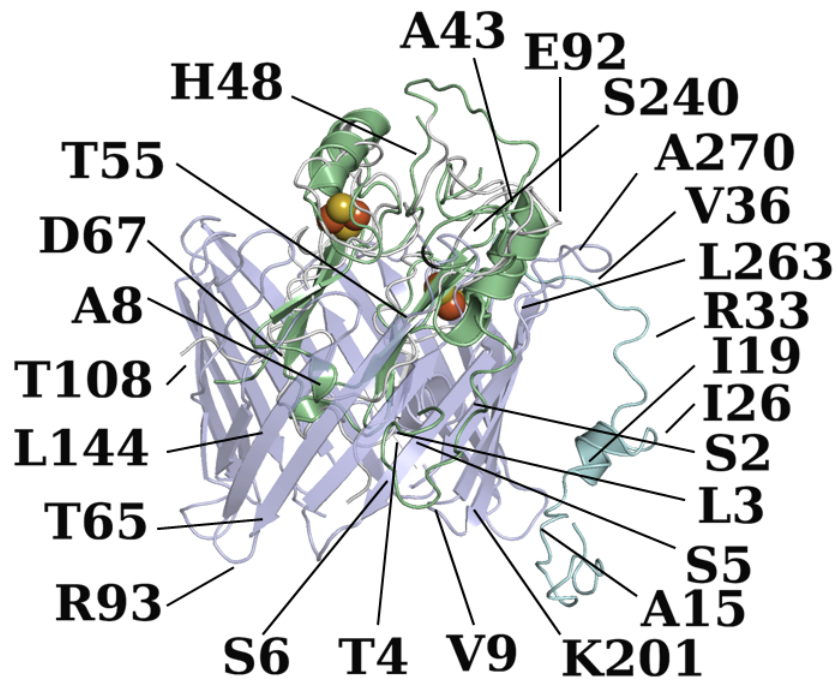


Figure S8: Model of mNT Docked to VDAC. The orientation of mNT within the VDAC pore was determined using Fd-DCA. Individual mNT monomers colored blue and green, with calculated direct-interacting residues from *Supplemental Table 1* labeled.

Supplemental Table 1. Top 20 DI-ranked pairs computed with DCA for interaction between mNT and VDAC.

Residue in mNT	Residue in VDAC	DI	Rank	Residue in mNT	Residue in VDAC	DI	Rank
9	55	1.0067	1	9	144	0.757	11
36	55	0.9503	2	2	55	0.756	12
3	55	0.9102	3	48	55	0.752	13
15	201	0.8463	4	6	8	0.741	14
36	144	0.845	5	43	55	0.715	15
26	55	0.8438	6	5	263	0.713	16
44	144	0.8051	7	4	8	0.707	17
92	270	0.7846	8	67	240	0.696	18
39	55	0.7579	9	108	65	0.688	19
33	55	0.7578	10	19	93	0.684	20

DCA, direct coupling analysis; DI, direct information.